ENHANCEMENT OF PARVALBUMIN INTERNEURON-MEDIATED NEUROTRANSMISSION IN THE RETROSPLENIAL CORTEX OF ADOLESCENT MICE FOLLOWING THIRD TRIMESTER-EQUIVALENT ETHANOL EXPOSURE

Clark W. Bird, Glenna J. Chavez, Megan J. Barber, and C. Fernando Valenzuela*

Department of Neurosciences, School of Medicine,
University of New Mexico Health Sciences Center
Albuquerque, New Mexico, USA

Corresponding Author: C. Fernando Valenzuela, M.D., Ph.D.
Department of Neurosciences
MSC08 4740
1 University of New Mexico
Albuquerque, NM 87131-0001
Phone (505) 272-3128
Fax (505) 272-8082
fvalenzuela@salud.unm.edu

ABSTRACT

Prenatal ethanol exposure causes a variety of cognitive deficits that have a persistent impact on quality of life, some of which may be explained by ethanol-induced alterations in interneuron function. Studies from several laboratories, including our own, have demonstrated that a single binge-like ethanol exposure during the third-trimester equivalent of human pregnancy leads to acute apoptosis and long-term loss of interneurons in the rodent retrosplenial cortex (RSC). The RSC is interconnected with the hippocampus, thalamus, and other neocortical regions and plays distinct roles in visuospatial processing and storage and retrieval of hippocampal-dependent episodic memories. Here we used slice electrophysiology to characterize the acute effects of ethanol on GABAergic neurotransmission in neonates, as well as the long-term effects of neonatal ethanol exposure on parvalbumin-interneuron mediated neurotransmission in adolescent mice. Mice were exposed to ethanol using vapor inhalation chambers. In postnatal day (P) 7 mouse pups, ethanol unexpectedly failed to potentiate $GABA_A$ receptor-mediated synaptic transmission. Binge-like ethanol exposure of P7 mice expressing channel rhodopsin in parvalbumin-positive interneurons enhanced the peak amplitudes, total charge, decays, and decreased rise-times of optically-evoked $GABA_A$ receptor-mediated inhibitory postsynaptic currents in adolescent animals. These effects could partially explain learning and memory deficits caused by developmental ethanol exposure.

INTRODUCTION

Exposure to ethanol during fetal development causes a spectrum of deficits, including growth retardation, craniofacial anomalies, and CNS alterations. Ethanol affects multiple developmental processes in the fetal brain, leading to long-lasting neurobehavioral alterations that can have a negative impact on the quality of life. Learning, memory, planning, judgement, attention, fine motor control, social interactions, sleep, and emotional control are among the myriad brain functions that can be disrupted by prenatal ethanol exposure. Studies indicate that dysfunction of GABAergic interneurons (INs) likely contributes to these neurobehavioral deficits. Moore et al[1,2] reported a reduction in the number of parvalbumin-expressing GABAergic INs (PV-INs) in the medial septum and anterior cingulate cortex of adult rats that were exposed to ethanol (peak blood ethanol concentration (BEC) = 160 mg/dl) via liquid diet during gestational days 0 to 21 (i.e., equivalent to the first and second trimesters of human pregnancy). Bailey et al[3] found a reduction in the number of glutamic acid decarboxylase immunopositive cells in layers II/III of the somatosensory cortex of adult guinea pigs that were exposed to ethanol (oral administration; peak BEC = 328 mg/dl) during the equivalent of all trimesters of human gestation. Miller[4] observed a reduction in the number of GABA-positive neurons in all layers (except for layer V) of the somatosensory and motor cortices of adolescent macaques that were exposed to ethanol (intragastric intubation; peak BEC = 230 mg/dl) during the first six weeks of gestation or throughout gestation (24 weeks). Cuzon et al[5] demonstrated that exposure of mice to a low dose of ethanol (liquid diet; peak BEC = 25 mg/dl) during the first 14.5 days of gestation induces premature GABAergic IN tangential migration into the cortical

anlage (detected at embryonic day 14.5), an effect that is mediated by increased ambient GABA levels and GABA sensitivity of migrating INs. Skorput et al[6] showed that 3-day binge-like ethanol exposure during embryonic days 13.5 and 16.5 (liquid diet; peak BEC = 80 mg/dl) increases the density of median ganglionic eminence-derived INs in 16.5-day-old embryos. This effect lingered until young adulthood, as evidenced by both an increase in the number PV-INs in layer V of the medial prefrontal cortex, as well as potentiation of $GABA_A$ receptor-mediated synaptic transmission at pyramidal neurons. The mechanism responsible for this effect of ethanol involves potentiation of the depolarizing action of $GABA_A$ receptors in migrating cells and increased neurogenesis in the medial ganglionic eminence[7,8]. Larsen et al[9] exposed differentiating human pluripotent stem cells to ethanol (50 mM for 50 days to model exposure during the first trimester of human gestation) and found a reduction in transcripts related to GABAergic IN specification (i.e., *GSX2, DLX1-6, SST,* and *NPY*) without effects on IN number. Collectively, these studies indicate that ethanol exposure during the equivalent to the first and second trimesters of human pregnancy causes dose- and region-specific effects on IN proliferation, differentiation, migration, and/or survival.

Ethanol exposure during the equivalent to the last trimester of human pregnancy has also been shown to have deleterious effects on INs. Exposure of rats to ethanol vapor (peak BEC = 206 mg/dl) between postnatal day (P) 2 and P6 caused an increase in the number of calretinin positive INs and a reduction in calbindin positive INs (with no change in PV-INs) in the primary motor and somatosensory cortex at P60[10]; this group of investigators also found a reduction in the dendritic tree of PV-INs in the striatum at P60[11]. Also using an ethanol vapor chamber paradigm (E12-19 and P2-9; peak BEC =

330 mg/dl at P7-8), Nirgudkar et al[12] found reductions in cerebellar IN numbers at P16. Bird et al[13] demonstrated that ethanol vapor exposure during P2-9 (peak BEC = 221 mg/dl) reduces IN numbers in the adult mouse hippocampus; this study also found that a single vapor chamber exposure at P7 (peak BEC = 297 mg/dl) increases the number of INs that express activated caspase-3, suggesting that they are programmed to undergo apoptotic neurodegeneration. Ethanol administration to P7 mice (subcutaneous injection; peak BEC near 500 mg/dl) has been shown to reduce the numbers of PV-INs in the frontal cortex at P82[14], as well as the hippocampal formation (at P14 and P90-100) and pyriform cortex (at P100)[15,16]. The same subcutaneous P7 ethanol administration paradigm has been demonstrated to decrease the numbers of PV and calretinin positive INs in the neocortex of adult mice[17]. It can be concluded from these results that INs are particularly sensitive targets of the effects of ethanol exposure during the third trimester-equivalent of human pregnancy.

We recently reported that P7 ethanol vapor administration (peak BEC = 400 mg/dl) triggers apoptotic neurodegeneration of INs in the retrosplenial cortex (RSC) of mice[18]. In the same study, we also found that acute bath application of ethanol to brain slices from P6-8 mice decreased the amplitude of both NMDA and non-NMDA glutamatergic excitatory postsynaptic currents; however, only inhibition of NMDA receptors affected synaptic excitability in RSC neurons. These results support the hypothesis that inhibition of NMDA receptors mediates the apoptogenic effects of third-trimester ethanol exposure[19-22]. Here, we tested whether this ethanol exposure paradigm causes either acute or long-lasting alterations in $GABA_A$ receptor-mediated neurotransmission in the RSC. We focused on this brain region because of its

importance for visuospatial memory and other cognitive processes. Specifically, to determine the acute effects of ethanol on $GABA_A$ receptors, we first bath applied ethanol to tissue slices from P6-8 pups and measured the effect of ethanol on evoked $GABA_A$ receptor-mediated postsynaptic currents. Next, to determine long-term effects of ethanol, we used optogenetic techniques in acute brain slices to investigate its impact on GABAergic transmission at PV-IN-to-pyramidal neurons synapses in young-adult mice.

METHODS

All procedures involving animals were approved by the Institutional Animal Care and Use Committee of the University of New Mexico Health Sciences Center and adhered to the U.S. Public health Service policy on humane care and use of laboratory animals. All chemicals were purchased from Sigma-Aldrich (St. Louis, MO) unless otherwise indicated.

Experiment 1

Animals

Transgenic mice expressing Venus yellow fluorescent protein in GABAergic and glycinergic INs expressing the vesicular GABA transporter (VGAT) were generously provided by Dr. Yuchio Yanagawa (Gunma University Graduate School of Medicine, Maebashi, Japan)[23]. Mice were housed at 22°C on a reverse 12-h light/dark cycle (lights on at 8 p.m.) with *ad libitum* access to standard chow and water. Both male and female pups P6-P8) were used for Experiment 1 (Figure 1a).

Slice electrophysiology

Slice electrophysiology experiments were performed as described previously[18]. Briefly, P6-P8 pups were anaesthetized with isoflurane (Piramal Critical Care, Bethelhem, PA) and rapidly decapitated. Brains were quickly removed and submerged for 3 min in a protective sucrose cutting solution. Ventral RSC-containing (equivalent to bregma -1.31 to -2.53 in an adult mouse[24]) coronal slices (300 µm) were prepared using a vibrating slicer (VT 1000S, Leica Mirosystems, Bannockburn, IL). Brain slices were then placed in a holding solution for 40 min at 32-34°C, followed by storage in a holding solution at room temperature (~24°C) for 30 min before recordings began. Recordings were acquired at 10 kHz and filtered at 2 kHz. Recordings were collected and analyzed using Clampex and Clampfit software (version 10 or 11; Molecular Devices, San Jose, CA), respectively.

Whole-cell patch-clamp recordings of both spontaneous $GABA_A$ receptor-mediated postsynaptic currents ($GABA_A$-sPSCs) and electrically-evoked $GABA_A$ receptor-mediated postsynaptic currents ($GABA_A$-ePSCs) were performed using an internal solution composed of (in mM): 140 Cs-methanesulfonate, 0.5 EGTA, 15 HEPES, 2 tetramethylammonium chloride, 2 Mg-ATP, 0.3 Na-GTP, 10 phosphocreatine disodium salt, and 4 QX-314-Cl (Hello Bio, Princeton, NJ) pH 7.25 (adjusted with CsOH) and 305 mOsm. Neurons were equilibrated with the internal solution for 5 min prior to recording. After the equilibration period, the holding potential was gradually increased from -70 mV to 0 mV in order to see $GABA_A$-PSCs. Recordings were obtained from pyramidal neurons (Venus negative) and INs (Venus positive) in layer V of the RSC.

Evoked PSCs were triggered with a concentric bipolar stimulating electrode (Catalog #CBAEC75, FHC, Bowdoin, ME) that was placed in layer II approximately 100 µm away from the cell being recorded from using a MP-225 micromanipulator (Sutter Instruments) (Figure 1a). Submaximal ePSCs were evoked with a Master-8 pulse stimulator (AMPI, Jerusalem, Israel) connected to an ISO-Flex stimulus isolator (AMPI) every 30 s using 75 µs square wave pulses. Recording of both sPSCs and ePSCs consisted of four phases: 10 min baseline, 10 min drug application, 10 min washout, and finally application of gabazine (25 µM; Hello Bio) to verify that PSCs were indeed $GABA_A$ receptor mediated. Kynurenic acid (3 mM) was applied during the equilibration and all recording phases to block excitatory glutamatergic activity. During the drug application phase, either 90 mM ethanol or 1 µM flunitrazepam (Research Biochemicals International, Natick, MA) were applied to the slice.

For sPSC recordings, the last 5 minutes of the baseline, 90 mM ethanol application, and washout phases were analyzed using the Mini Analysis Program (Synaptosoft, Decatur, GA). For ePSC recordings, an input/output curve was initially measured and the stimulation intensity was subsequently adjusted so that the ePSC amplitude was 30-40% of the maximum amplitude. PSCs were evoked at 0.033 Hz. Amplitudes were normalized to the average amplitude of the sPSCs from the entire baseline phase. For ePSCs, both normalized amplitude and decay constant tau were measured during the last 3 minutes of each recording phase for both 90 mM ethanol and 1 µM flunitrazepam application experiments. Tau was calculated by averaging the ePSC waveforms from the last 3 minutes of each phase and fitting the resulting trace with a single exponential decay function.

Experiment 2

Animals

Mice expressing the channel rhodopsin-2 (ChR2) variant ChR2 H134R fused to tdTomato in PV-INs were generated by crossing female heterozygous B6.129P2-Pvalb$^{tm1(cre)Arbr}$/J (B6 PV^{cre}, Jackson Laboratory, Bar Harbor, ME; stock number 017320) and male heterozygous B6.Cg-Gt(ROSA)26Sor$^{tm27.1(CAG-COP4*H134R/tdTomato)Hze}$/J (Ai27D, Jackson Laboratory; stock number 012567) mice. After weaning, the offspring (hereafter referred to as B6 PV^{cre}-Ai27D mice) were ear-tagged and tail snips were collected under isoflurane anesthesia. Genotyping was performed by Transnetyx (Cordova, TN). Male and female mice aged between P40 and P60 were used for all subsequent experiments (Figure 1b).

Ethanol vapor chamber exposure

Pups and dams were exposed to either air or vaporized ethanol (95%, Koptec, King of Prussia, PA) for 4 h (approximately 10 a.m. to 2 p.m.) at P7 in custom-built ethanol vapor chambers[25]. Ethanol vapor concentrations were determined using a breathalyzer (Intoximeters, St. Louis, MO) and were between 8-9 g/dl. This exposure paradigm produces peak BECs in pups near 80 mM and triggers apoptotic neurodegeneration in several brain regions, including the RSC[13,18].

Immunohistochemistry

Tissue sections were stained with an anti-PV antibody to verify both the specificity and penetrance of ChR2- H134R/tdTomato expression. Immunohistochemistry (IHC) experiments were performed as described previously[13]. Male and female B6 PV^{cre}-Ai27D mice aged P40-60 that were exposed to either air or vaporized ethanol at P7 were deeply anaesthetized with ketamine (250 mg/kg intraperitoneally), the diaphragm was sectioned, and brains were transcardially perfused with 4% paraformaldehyde (PFA, 4% w/v in phosphate buffered saline (PBS), pH 7.4). Brains were extracted and stored in 4% PFA for 48 h, before being cryoprotected for 48 h in 30% sucrose (w/v in PBS). Brains were frozen at -80°C until sectioning. Parasagittal sections (50 µm) were prepared using a cryostat (Microm 505E, Waldorf, Germany). Floating sections were stored at -20°C in a cryoprotectant solution (0.05 M phosphate buffer pH 7.4, 25% glycerol and 25% ethylene glycol). Five randomly selected parasagittal sections (from both hemispheres) containing the ventral RSC were incubated for 2 h in 1% bovine serum albumin, 0.2% Triton X-100, and 5% donkey serum (Jackson ImmunoResearch, West Grove, PA) in PBS (pH 7.4). The sections were next incubated with a 1:5,000 dilution of anti-PV monoclonal antibody (catalog # 235, Swant Inc., Switzerland) at 4°C. Sections were then incubated in a secondary antibody solution containing a 1:1000 dilution of donkey anti-mouse IgG Alexa Fluor™ 488 antibody (catalog # A21202, Thermo-Fisher, Waltham, MA,) for 2 h at room temperature (approximately 23°C), and then for 20 min in 600 nM 4'6-diamidino-2-phenylindole hydrochloride (DAPI). Sections were rinsed with PBS and mounted on Superfrost Plus microscope slides (VWR, Radnor, PA) using Fluromount G mounting media (Southern Biotech, Birmingham, AL) and covered with glass coverslips (VWR).

Sections were imaged using a Nuance spectral imaging system (PerkinElmer, Hopkinton, MA) on a Nikon TE-200 U inverted fluorescence microscope (Nikon Instruments Inc., Melville, NY) as described previously[18]. Images were acquired with a 40X objective (Plan-NEOFLUAR 40X/1.3 oil, Zeiss, White Plains, NY). The number of Alexa-Fluor 488 stained PV positive cells (525 nm emission maximum), the number of cells expressing tdTomato (581 nm emission maximum), and the number of cells positive for both for Alexa-Fluor 488 and tdTomato were exhaustively counted in Layer V of the ventral RSC in each section by an experimenter blinded to the experimental conditions. For each animal, the percentage of PV positive cells colocalized with tdTomato were ascertained as a measure of transgene penetrance (i.e., number of PV+ cells colocalized with tdTomato divided by the number of PV+ cells), and the percentage of cells expressing tdTomato that did not express PV was determined as a measure of transgene specificity (i.e, number of cells expressing only tdTomato without PV divided by the number of PV+ cells colocalized with tdTomato). Cells were counted using the point selection tool in Fiji (NIH Image J software[26]).

Optogenetic slice electrophysiology

Electrophysiology experiments were performed using the same methods as described in Experiment 1 with the modifications detailed below. Slices were prepared from male and female B6 PV^{cre}-Ai27D mice aged P40-P60 using the protective cutting/recovery methodology of Ting et al[27]. Mice were deeply anaesthetized with ketamine (250 mg/kg intraperitoneally) and transcardially perfused with 25 mL of a protective N-methyl-D-glucamine (NMDG)-containing aCSF at 4°C composed of (in

mM): 92 NMDG, 2.5 KCl, 1.25 NaH_2PO_4, 30 $NaHCO_3$, 20 HEPES, 25 glucose, 2 thiourea, 3 sodium pyruvate, 5 ascorbic acid, 10 $MgSO_4$, and 0.5 $CaCl_2$ saturated with 95% O_2/5% CO_2 (pH 7.3-7.4 with HCl; 300-310 mOsm). Brains were rapidly removed and immersed for 1 min in the same NMDG-containing aCSF. Coronal brain slices (300 µM) were prepared using the vibrating slicer (described above under Experiment 1) in NMDG aCSF at 4°C. Once all slices containing the ventral RSC (bregma -1.31 to -2.53[24]) were prepared, they were transferred to warm NMDG aCSF holding solution at 32-34°C. Over the course of 25 min, the NaCl concentration of the warm holding solution was gradually increased to 52 mM by adding increasing amounts of NMDG-aCSF containing 2M NaCl. Slices were then allowed to recover in holding solution at room temperature for 1 h (as described for Experiment 1 above).

Following recovery, slices were transferred to the recording chamber and aCSF containing 3 mM kynurenic acid was applied at a rate of 2 ml/min. Recording electrodes were filled with the same Cs-methanesulfonate internal solution used in Experiment 1. Optically-evoked PSCs (oIPSCs) were generated in layer V pyramidal neurons using a 473 nm laser (IKE-473-100-OP) connected to a power supply (IKE PS-300) (IkeCool Corporation, Anaheim, CA) (Figure 1b). Laser light was delivered through the 40X objective lens using an IS-OGP optogenetics laser positioner (Siskyou, Grants Pass, OR). Laser output power was 20 mW. Cellular capacitance and membrane resistance were measured immediately before recordings began. Three oIPSCs at 20 seconds intervals were generated at each of the following laser pulse durations: 0.5 ms, 1 ms, 2 ms, 4 ms, and 8 ms. The oIPSC was then blocked with gabazine (25 µM) to confirm that the oIPSC was a GABA mediated current. Data from any cell with an oIPSC that was

not blocked with gabazine was discarded. The average oIPSC at each laser pulse duration for every cell was analyzed for peak amplitude, GABAergic total charge (area under the curve, pA X ms), half-width at half-maximal amplitude, rise time, and decay time using Clampfit (Molecular Devices). The decay constant tau was measured for each oIPSC using the Mini Analysis Program (Synaptosoft). To measure oIPSC paired pulse ratios (PPRs), we evoked 10 pairs of oIPSCs at 30 s intervals, with 50 ms between paired laser pulses and 1 ms laser pulse durations. The ratio of the amplitude or the total charge of the second peak divided by the first peak (P2/P1) was measured.

Statistics

Statistical analyses were performed using Prism version 8.4.2 (GraphPad Software, San Diego, CA) and SPSS version 26 (IBM, Armonk, NY). Precise p-values are reported as recommended by a recent article[28]. Data from Experiment 1 were analyzed using repeated measures ANOVA with cell-type (pyramidal or IN) as the fixed factor and the three phases (baseline, drug application, washout) as the repeated measure. ANOVA residuals were tested for normality using a Shapiro-Wilkes test, and any data that failed this test ($p < 0.05$) was analyzed using a non-parametric Friedman's ANOVA test. Since Experiment 1 examined the acute effect of ethanol or flunitrazepam on PSCs, the unit of determination was a single cell. For ePSCs, the dependent measure was either evoked current amplitude or decay (tau). For sPSCs, the dependent measures were frequency, amplitude, rise time, and decay (tau). Main effect of cell-type for non-parametric data was analyzed using a Mann-Whitney U test. F-ratios and p-values are reported for cell-type, phase, and cell-type by phase interactions for all

dependent variables. Greenhouse-Geisser corrected F-ratios and p-values are reported for repeated measures that failed ($p < 0.05$) Mauchley's test of sphericity. Any cell-type X phase interactions were further explored by performing a multiple comparison test within cell type, comparing the baseline, drug-application and washout in a pairwise manner. Bonferroni corrected p-values are reported for all multiple comparison tests. Effect sizes for Experiment 1 are reported as follows: partial eta squared (η_p^2) for ANOVAs, Kendall's *W* for Friedman's ANOVA, Hedge's *g* for pairwise multiple comparison post hoc tests, and *r* for Friedman's ANOVA post hoc multiple comparisons and Mann-Whitney U tests.

IHC data from Experiment 2 was analyzed using an unpaired t-test for parametric data or a Mann-Whitney U test for non-parametric data. Effect sizes for these tests are reported as Hedges' *g* or *r,* respectively. For optogenetic electrophysiology experiments from Experiment 2, because multiple cells were recorded from several animals from several litters, we used a linear mixed-model (LMM) approach to data analysis in SPSS adapted from procedures described by West et al[29]. This approach allows us to determine if including random litter effects significantly improves the linear mixed-model being used for a particular dependent variable[30]. Detailed statistics from LMM analyses appear in Supplemental Table 2. Before LMM analyses were performed, outliers for each dependent variable were removed using a 1% ROUT test in GraphPad. The fixed factors were sex, P7 vapor chamber exposure condition, and laser pulse duration as a repeated measure. Models were built stepwise for each dependent variable according to the following procedure. First, a LMM was fit that includes the random effect associated with the intercept for each litter, using homogenous residual error variances

between treatment groups, and an unstructured covariance structure for the repeated measures residuals. If the LMM failed to achieve convergence using an unstructured covariance structure for repeated measures residuals, a compound symmetry covariance structure was used instead. Then a LMM was fit without the random effect included. The -2-log restricted maximum likelihood value for each model fit was then used to perform a likelihood ratio chi-square test. If the p-value for this test was < 0.05, this indicated that random effects significantly improved the model fit and were therefore included in subsequent models. The resulting LMM was then fit using heterogenous residual error variances for treatment groups, and another likelihood ratio chi-square test was performed. If the p-value for this test was < 0.05, including heterogenous residual error variances significantly improved the model and subsequent LMMs included heterogenous residual error variances. F-ratios (containing Satterthwaite approximated degrees of freedom) and p-values for Type III F-tests for treatment, sex, laser pulse duration, and interactions between fixed factors from the final LMM are reported in the results section for each dependent variable. Effect sizes for main effects of exposure and sex for LMMs are reported as Hedges' *g* and not partial eta squared because SPSS currently does not provide a sum of squares output for these tests. Some skewness and kurtosis in data distribution can be tolerated using LMMs as they are robust against violations of assumptions of normality, as normality of residuals does not affect parameter estimates in multilevel models[31]. However, because residuals from many of the LMMs violated assumptions of normality (Shapiro-Wilkes p-value of < 0.05), we also present non-parametric Mann-Whitney U tests for main effects of vapor chamber exposure condition and sex in Supplemental Table 2 for any LMM that did not

pass the Shapiro-Wilkes test. Exposure by laser pulse duration interactions with a p-value of < 0.05 were subsequently analyzed with non-parametric Mann-Whitney U tests examining the effect of vapor chamber exposure condition within each laser pulse duration. P-values reported for these tests are Bonferroni corrected. Sex X exposure interactions with a p-value of < 0.05 were further analyzed by performing a LMM examining exposure and laser pulse duration effects within sex, including random effect of litter and heterogenous residual error variances if they were also included in the parent LMM. All p-values from these post hoc LMMs are also Bonferroni corrected. Exposure by laser pulse duration interactions within sex were subsequently analyzed with post hoc Mann-Whitney U tests examining the effect of vapor chamber exposure condition within each laser pulse duration. Detailed statistics for post hoc tests examining exposure effects within each laser pulse duration appear in Supplemental Table 3. All data presented are mean ± standard error of the mean (SEM).

RESULTS

Experiment 1: Effects of acute ethanol exposure on $GABA_A$ receptor-mediated PSCs in the RSC

In our previous work[18], we demonstrated that bath application of 90 mM ethanol to acutely prepared brain slices from P6-P8 pups inhibited NMDA and non-NMDA receptor-mediated excitatory postsynaptic currents in both pyramidal neurons and INs from layer V of the RSC. This concentration is above the threshold of BECs required for the induction of apoptotic neurodegeneration in postnatal rodents [13,18,20]. In this work, we sought to determine the effects of bath-applied ethanol on $GABA_A$-ePSCs in

pyramidal neurons and INs in the same region. We hypothesized that ethanol acutely potentiates $GABA_A$ receptors, which could contribute to apoptosis caused by excessive inhibition of neuronal activity. We applied 90 mM ethanol to acutely prepared brain slices from male and female mice at P6-P8. We elicited submaximal $GABA_A$-ePSCs in layer V pyramidal neurons and INs using a bipolar stimulating electrode placed in layer II (Figure 1a). Average traces from pyramidal neurons and INs obtained during the baseline and 90 mM ethanol exposure phases appear in Figures 2a and 2b, respectively. Contrary to our expectations, acute bath application of 90 mM ethanol failed to potentiate $GABA_A$-ePSC amplitudes in either pyramidal neurons or INs in layer V of the RSC (Figure 2c). Using a repeated-measures two-way ANOVA, we observed an effect of exposure phase, with amplitudes decreasing over the course of the experiment instead of increasing during the 90 mM ethanol exposure phase (phase $F(2,32) = 3.976$, $p = 0.029$, $\eta_p^2 = 0.199$; male pyramidal n = 4 cells from 4 animals from 2 litters, female pyramidal n = 6 cells from 5 animals from 4 litters; male IN n = 4 cells from 4 animals from 2 litters; female IN n = 4 cells from 4 animals from 3 litters). This effect of phase was driven by a gradual decrease in the $GABA_A$-ePSC amplitude over time (post hoc baseline vs. wash $t(32) = 2.797$, $p = 0.026$, $g = 0.753$). There was no effect of cell type examined (cell type $F(1,16) = 3.442$, $p = 0.082$, $\eta_p^2 = 0.177$), or interaction between exposure phase and cell type (interaction $F(2,32) = 1.932$, $p = 0.16$, $\eta_p^2 = 0.108$).

Although ethanol does not potentiate $GABA_A$-ePSCs in RSC neurons by increasing current amplitude, it may increase the decay time of the current, allowing for more total current flow into the postsynaptic cell. Therefore, $GABA_A$-ePSCs were fit with

a single exponential decay curve, and the decay constant tau was measured. Bath application of 90 mM ethanol failed to affect the decay constant of $GABA_A$-ePSCs in either cell type examined (Figure 2d). There was an effect of phase (Friedman's ANOVA $\chi^2(2) = 11.444$, $p = 0.003$, $W = 0.318$) which was driven by a decrease in the decay constant during the washout phase compared to the 90 mM exposure phase (Friedman's ANOVA post hoc 90 mM ethanol vs wash p-value = 0.0026, $r = 0.556$). There was no effect of cell type examined (Mann-Whitney U (n1 = 10, n2 = 8) = 33, p = 0.58, $r = 0.147$).

After observing that 90 mM ethanol application did not potentiate $GABA_A$-ePSCs in either pyramidal neurons or INs in layer V of the RSC, we confirmed that it was possible to potentiate $GABA_A$-ePSCs in these developing neurons. To this end, we performed the same experiment described above using the allosteric potentiator of $GABA_A$ receptors, flunitrazepam (1 µM). Flunitrazepam is a benzodiazepine that has been demonstrated to increase decay time of $GABA_A$-PSCs (Bouairi et al., 2006). Average traces during the baseline and 1 µM flunitrazepam application phases for pyramidal neurons and INs appear in Figure 3a and Figure 3b, respectively. Application of 1 µM flunitrazepam did not increase the amplitude of the ePSCs from either cell type (phase $F(1.602,41.650) = 2.757$, $p = 0.86$, $\eta_p^2 = 0.096$; cell type $F(1,26) = 0.066$, $p = 0.80$, $\eta_p^2 = 0.003$; interaction $F(2,52) = 0.042$, $p = 0.96$, $\eta_p^2 = 0.002$; male pyramidal n = 9 cells from 6 animals from 4 litters; female pyramidal n = 5 cells from 3 animals from 3 litters; male IN n = 10 cells from 6 animals from 4 litters; female IN n = 4 cells from 2 animals from 2 litters) (Figure 3c).

Flunitrazepam application, however, increased $GABA_A$-ePSC decays in both cell types. The decay constant tau was elevated in both cell types during the 1μM flunitrazepam application phase, and this potentiation continued into the washout phase (Figure 3d). There was an effect of phase (phase $F(1.699, 44.190) = 58.91$, $p < 0.001$, $\eta_p^2 = 0.694$), but no differences between cell types (cell type $F(1,26) = 3.205$, $p = 0.085$, $\eta_p^2 = 0.110$) or interaction between phase and cell type (interaction $F(2,52) = 1.565$, $p = 0.22$, $\eta_p^2 = 0.057$). These results indicate that $GABA_A$ receptors on layer V pyramidal neurons and INs in the RSC of P6-P8 animals can be potentiated by drugs that allosterically modulate $GABA_A$ receptor function but that 90 mM ethanol does not potentiate evoked $GABA_A$ receptor activity. Therefore, it is unlikely that acute apoptosis resulting from ethanol exposure at this critical developmental age is a result of potentiation of inhibition via $GABA_A$ receptors.

To more thoroughly determine that 90 mM ethanol application did not have any potentiating effects on $GABA_A$ receptor-mediated synaptic transmission in layer V pyramidal neurons and INs, we recorded $GABA_A$-sPSCs during the baseline, 90 mM ethanol bath application, and washout phases. Representative $GABA_A$-sPSC traces for pyramidal neurons and INs during the baseline and 90 mM ethanol application phases appear in Figures 4a and 4b, respectively. We measured the sPSC frequency, amplitude, rise time (10-90%) and single-exponential decay constant tau during each of the phases for the two cell types. Mean values with standard errors for these dependent variables in both pyramidal neurons and INs during the three phases of the experiment appear in Table 1 (male pyramidal n = 4 cells from 4 animals from 4 litters; female pyramidal = 4 cells from 4 animals from 3 litters; male IN = 4 cells from 4 animals from 4

litters, female IN = 3 cells from 3 animals from 2 litters). There was no effect of exposure phase on frequency of $GABA_A$-sPSCs (phase $F(1.382,17.970) = 3.485$, $p = 0.067$, $\eta_p^2 = 0.211$), and no phase by cell type interaction ($F(1.382,17.970) = 0.345$, $p = 0.63$. $\eta_p^2 = 0.026$). Pyramidal neuron $GABA_A$-sPSCs occurred more frequently than IN $GABA_A$-sPSCs (cell type $F(1,13) = 9.980$, $p = 0.0075$, $\eta_p^2 = 0.434$). There was an effect of exposure phase on the amplitude of $GABA_A$-sPSCs (phase $F(1.336,17.371) = 4.913$, $p = 0.031$, $\eta_p^2 = 0.274$) and an interaction between exposure phase and cell type (interaction $F(1.336,17.371) = 6.108$, $p = 0.017$, $\eta_p^2 = 0.320$), but no effect of cell type examined (cell type $F(1,13) = 0.137$, $p = 0.72$, $\eta_p^2 = 0.010$). The effect of phase and the interaction between phase and cell type was primarily driven by an increase in IN $GABA_A$-sPSC amplitude during the washout phase as compared to the baseline phase, but this effect was not observed using a multiple comparison post hoc test ($t(6) = 2.357$, $p = 0.17$, $g = 0.856$). There were no effects on $GABA_A$-sPSC rise time (phase $F(2,26) = 2.763$, $p = 0.082$, $\eta_p^2 = 0.175$; cell type $F(1,13) = 1.448$, $p = 0.25$, $\eta_p^2 = 0.100$; interaction $F(2,26) = 0.265$, $p = 0.77$, $\eta_p^2 = 0.020$). There was also no effect of exposure phase or interaction between exposure phase and cell type on $GABA_A$-sPSC decay tau (phase $F(2,24) = 0.834$, $p = 0.45$, $\eta_p^2 = 0.065$; interaction $F(2,24) = 0.123$, $p = 0.89$, $\eta_p^2 = 0.010$). INs had a higher tau value than pyramidal neurons, indicating that $GABA_A$-sPSCs decayed more slowly in INs than pyramidal cells (cell type $F(1,12) = 13.543$, $p = 0.0031$, $\eta_p^2 = 0.530$).

Experiment 2: Long-term effects of P7 ethanol vapor chamber exposure on oIPSCs in layer V pyramidal neurons in the ventral RSC

Third trimester-equivalent ethanol exposure has been shown to trigger apoptosis and long-term loss of INs, including PV+ INs, in the RSC[18,32], which could lead to persistent alterations in GABAergic neurotransmission. To examine this possibility, we used a transgenic mouse model (B6 PV^{cre}-Ai27D mice) that allowed us to optically stimulate PV+ INs specifically. We assessed whether PV+ IN-mediated oIPSCs in RSC layer V pyramidal neurons of adolescent mice are affected by P7 developmental ethanol exposure. We first determined the penetrance and specificity of transgene expression before starting electrophysiology experiments. We also determined if P7 ethanol exposure altered either of these measures. Male and female mice from both P7 vapor chamber exposure conditions were left undisturbed until P40-P60 and then processed for immunohistochemistry to analyze both PV expression and ChR2/tdTomato expression. Representative IHC images from B6 PV^{cre}-Ai27D mice appear in Figure 5 a-d. In air exposed animals, mean transgene penetrance was 98.67 ± 1.33% (percentage of PV+ cells expressing ChR2-tdTomato), while in ethanol exposed animals transgene penetrance was 98.82 ± 1.18% (Figure 5e; air male n = 3 animals from 3 litters, air female n = 2 animals from 2 litters; ethanol male n = 3 animals from 3 litters, ethanol female n = 2 animals from 2 litters). Transgene penetrance was not different between vapor-chamber exposure conditions (Mann-Whitney U(n1 = n2 = 5) = 12, p > 0.99, *r* = 0.047). We also measured transgene specificity to see if ChR2-tdTomato was aberrantly expressed in PV-negative cells. In air exposed animals, non-specific transgene expression (% of ChR2-tdTomato positive cells that were not positive for PV) was 3.76 ± 1.58%, while in ethanol exposed animals non-specific transgene expression

was 4.81 ± 2.05% (Figure 5f). Transgene specificity was not different between vapor chamber exposure conditions ($t(8) = 0.406$, $p = 0.70$, $g = 0.232$).

After verifying that B6 PV^{cre}-Ai27D mice had acceptable transgene expression, we then examined the effect of P7 ethanol exposure, sex, and laser pulse duration on PV+ IN-mediated oIPSCs in layer V pyramidal neurons in the RSC of both male and female mice at P40-P60 using whole-cell patch-clamp electrophysiology. Average oIPSC traces from each laser pulse duration for mice from air and ethanol vapor chamber exposure conditions appear in Figure 6a and 6b, respectively (female air n = 32 cells from 8 animals from 7 litters; male air n = 46 cells from 9 animals from 8 litters; female ethanol n = 35 cells from 8 animals from 8 litters; male ethanol n = 40 cells from 8 animals from 7 litters). There was no effect of vapor chamber exposure condition, sex, or interaction between sex and exposure condition on membrane capacitance (p-values > 0.07, Supplemental Figure 1a). There was no effect of vapor chamber exposure condition or interaction between exposure condition and sex on membrane resistance (p-values > 0.39; Supplementary Figure 1b), but females did have a larger membrane resistance than males ($F(1,95.267) = 4.199$, $p = 0.043$, $g = 0.498$ (Supplemental Figure 1b). Random effect of litter significantly improved the LMM for membrane resistance and was included in the final model; random effect of litter did not significantly improve the LMM for membrane capacitance and was not included in the final model.

Peak amplitude of oIPSCs was increased by vapor-chamber exposure condition (Figure 6c; exposure $F(1,146.828) = 5.009$, $p = 0.027$, $g = 0.328$). Peak amplitude was also affected by laser pulse duration (laser $F(4,138.866) = 73.641$, $p < 0.0001$) There was no effect of sex, or two- or three-way interactions between sex, exposure, and laser

pulse duration on oIPSC amplitude (p-values > 0.08). Random effect of litter did not significantly improve the LMM for oIPSC amplitude and was not included in the final model.

Current density of oIPSCs was also increased in ethanol exposed animals (Figure 6d; exposure $F(1,40.564) = 4.044$, $p = 0.051$, $g = 0.384$). Laser pulse duration also affected current density (laser $F(4,38.243) = 66.409$, $p < 0.0001$). There was no effect of sex, or two- or three-way interactions between sex exposure, and laser pulse duration on oIPSC current density (p-values > 0.29). Random effect of litter significantly improved the LMM for oIPSC current density and was included in the final model.

The total charge of the oIPSCs was affected by vapor chamber exposure condition. Ethanol exposed animals had a larger oIPSC total charge than air-exposed animals (Figure 6e; exposure $F(1,20.848) = 5.907$ $p = 0.024$, $g = 0.424$). Laser pulse duration also affected oIPSC total charge (laser $F(4,88.351) = 133.734$, $p < 0.0001$). There was no effect of sex, or interactions between sex and exposure, sex and laser pulse duration, or sex by exposure by laser pulse duration interactions (p-values > 0.23). An exposure by laser pulse duration interaction ($F(4,88.351 = 2.849$, $p = 0.028$) was further explored by running Mann-Whitney U tests for exposure effects within each laser pulse duration for total charge. After correcting for multiple comparisons, there was an effect of vapor chamber exposure condition on total charge at the each of the laser pulse durations (all p-values < 0.024, for detailed statistics please see Supplementary Table 3). Random effect of litter for oIPSC total charge significantly improved the LMM and was included in the final model.

The half-width at half-maximal amplitude was not affected by exposure condition (Figure 6f; exposure $F(1,26.478) = 2.315$, $p = 0.14$, $g = 0.270$), but was affected by laser pulse duration (laser $F(4,40.164 = 51.786$, $p < 0.0001$). There was no effect of sex or interactions between sex, exposure, and laser pulse duration on oIPSC half-width (p-values > 0.32). Random effect of litter significantly improved the LMM for half-width and was included in the final model.

Ethanol vapor chamber exposure decreased the rise time (10-90%) of oIPSCs compared to air-exposed animals (Figure 6g; exposure $F(1,110.583) = 11.906$, $p = 0.0008$, $g = 0.359$). Laser pulse duration also affected oIPSC rise time (laser $F(4,102.143) = 15.353$, $p < 0.0001$). An exposure by laser pulse duration interaction was further explored using Mann-Whitney U tests for exposure effects within laser pulse duration, but after correcting for multiple comparisons there were no effects (p-values > 0.09; Supplemental Table 3). There was no effect of sex or other interactions between sex, vapor chamber exposure condition, and laser pulse duration for oIPSC rise time (p-values > 0.13). Random effect of litter did not significantly improve the LMM for oIPSC rise time and was not included in the final model.

Ethanol exposure at P7 prolonged the decay time (90-10%) of oIPSCs compared to air-exposed animals (Figure 6h; exposure $F(1,46.631) = 12.115$, $p = 0.0011$, $g = 0.476$). Laser pulse duration also affected decay time (laser $F(4,70.17) = 99.684$, $p < 0.0001$). There was an interaction between exposure and laser pulse duration for oIPSC decay time ($F(4,70.017) = 2.478$, $p = 0.052$), but this was not further explored with post hoc testing as it failed to meet the p-value threshold for post hoc testing established in the methods. There was no effect of sex or other interactions between sex, exposure,

and laser pulse duration on oIPSC decay time (p-values > 0.21). Random effect of litter significantly improved the LMM for oIPSC decay time and was included in the final model.

Similar to decay time, the decay constant tau was elevated in ethanol-exposed animals (Figure 6i; exposure $F(1,144.178) = 6.388$, $p = 0.013$, $g = 0.267$). Laser pulse duration also affected oIPSC decay tau (laser $F(4,141.952) = 49.034$, $p < 0.0001$). There was a sex by exposure effect for oIPSC decay tau ($F(1,144.178) = 6.459$, $p = 0.012$) that was further explored by running LMMs for decay tau within sex (using Bonferroni corrected p-values). Average oIPSC current traces for each laser pulse duration from air- and ethanol-exposed female mice appear in Supplemental Figures 2a and 2b, respectively. In females there was an effect of laser pulse duration (Supplemental Figure 2e; laser $F(4,61.763) = 23.305$, $p < 0.0001$), but no effect of exposure or interaction between exposure and laser pulse duration (p-values > 0.99). Average oIPSC current traces for each laser pulse duration from air- and ethanol-exposed male mice appear in Supplemental Figures 2c and 2d, respectively. In males, P7 ethanol exposure increased oIPSC decay tau compared to air-exposed animals (Supplemental Figure 2f; exposure $F(1,79.377) = 15.847$, $p = 0.0003$, $g = 0.506$). Male decay tau was also affected by laser pulse duration (laser $F(4,80.212) = 26.923$, $p < 0.0001$), and there was a exposure by laser pulse duration interaction ($F(4,80.212) = 3.666$, $p = 0.017$) that was further explored using Mann-Whitney U post hoc tests for exposure effects within each laser pulse duration (Supplemental Table 3). Ethanol exposure increased decay tau at the 1 ms ($U(n1 = 40, n2 = 39) = 293$, $p < 0.0001$, $r = 0.537$) and the 2 ms ($U(n1 = 43, n2 = 39) = 484$, $p = 0.0050$, $r = 0.364$) laser pulse

durations, but not at the 0.5, 4 and 8 ms durations (p-values > 0.10). Random effect of litter was not included in the post-hoc LMMs within sex for decay tau because they were not included in the parent LMM containing both sexes.

We next analyzed if P7 vapor chamber exposure altered GABA release at PV+ IN- pyramidal neuron synapses. We analyzed oIPSC PPRs in RSC layer V pyramidal neurons. Average PPR current traces from air and ethanol exposed animals show that paired-pulse depression was observed at these synapses, indicating that they have a high basal probability of GABA release (Figure 7a; Air female n = 19 cells from 5 animals from 4 litters, air male n = 22 cells from 6 animals from 5 litters; ethanol female n = 22 cells from 6 animals from 5 litters; ethanol male n = 20 cells from 5 animals from 5 litters). However, ethanol exposure at P7 had no effect on amplitude PPR ratios (Figure 7b; exposure $F(1,79) = 0.377$, $p = 0.54$, $g = 0.159$). Female mice had larger PPRs for amplitude than male mice, suggesting that females have a lower basal probability of GABA release (sex $F(1,79) = 5.119$, $p = 0.026$, $g = 0.507$). There was no interaction between sex and exposure condition for amplitude PPR (interaction $F(1,79) = 0.169$, $p = 0.68$). Similar to amplitude PPR, ethanol exposure had no effect on total charge PPR ratios (Figure 7c, exposure $F(1,79) = 1.521$, $p = 0.22$, $g = 0.291$), females had larger charge PPR ratios than male mice (sex $F(1,79) = 5.667$, $p = 0.034$, $g = 0.489$), and there was no interaction between sex and exposure condition (interaction $F(1,79) = 0.182$, $p = 0.67$). Random effect of litter did not improve the LMM for either amplitude PPR or total charge PPR and were not included in the final model. These data suggest that the long-lasting alterations in oIPSC characteristics caused by P7 ethanol exposure are not due to presynaptic effects.

DISCUSSION

The results of our study advance knowledge of the short- and long-term effects of developmental ethanol exposure on $GABA_A$ receptor-mediated transmission in the cerebral cortex. We demonstrate that acute ethanol exposure does not affect $GABA_A$ receptor function in the RSC of neonatal mice, suggesting that potentiation of these receptors is not involved in the mechanism responsible for the apoptotic neurodegeneration triggered by binge-like ethanol exposure during the brain growth spurt. Moreover, we show that this ethanol exposure paradigm causes long-lasting functional alterations at PV-IN→pyramidal neuron synapses from adolescent mice. These findings identify a novel mechanism that could contribute to the cognitive alterations associated with fetal alcohol spectrum disorder (FASD).

In Experiment #1, we demonstrate that $eGABA_A$-PSCs in layer V neurons of the mouse RSC are not affected by acute ethanol exposure during the third trimester-equivalent of human pregnancy. These results follow up on those of a recent study from our laboratory, in which we showed that acute exposure to ethanol during P6-P8 inhibits the excitability of RSC layer V pyramidal neurons and INs mainly through effects exerted post-synaptically on NMDA receptors[18]. Together, the outcomes of these two studies suggest that apoptosis caused by binge-like exposure to ethanol in the RSC during this critical developmental period is caused by inhibition of neuronal activity mediated by a decrease in the function of NMDA receptors, rather than potentiation of Cl^- current flow through $GABA_A$ receptors.

One of the hypotheses to explain why ethanol induces apoptotic neurodegeneration during the third trimester equivalent was developed by John Olney and colleagues about 20 years ago, after observing that patterns of cell death in the neonatal brain caused by ethanol exposure were similar to those produced by the non-competitive NMDA receptor antagonist, MK-801 and the $GABA_A$ receptor positive allosteric modulator, phenobarbital[20]. These investigators concluded that ethanol causes neurodegeneration via excessive inhibition of neuronal activity triggered by both NMDA receptor inhibition and $GABA_A$ receptor potentiation. Although a number of studies have demonstrated that ethanol can potentiate post-synaptic $GABA_A$ receptors under some conditions, there is substantial evidence indicating that the function of these receptors is not directly enhanced by ethanol in many neuronal populations; rather, an increase in GABA release appears to play a central role in the GABA-mimetic effect of ethanol (reviewed in [33] and [34]). This also appears to be the case for developing neurons during the brain growth spurt, as indicated by electrophysiological studies with slices from neonatal rats showing that acute ethanol increases GABA release while having minimal effects on postsynaptic $GABA_A$ receptor function in layer II and III pyramidal neurons of the parietal cortex[35], pyramidal neurons and INs of the CA3 hippocampal region[36,37], and hypoglossal motoneurons in the brain stem[38]. In contrast to the findings of these studies, we found that ethanol does not affect the amplitude of electrically evoked $GABA_A$-PSCs in RSC pyramidal neurons and INs. As a positive control, we measured the effect of flunitrazepam on e$GABA_A$-PSCs and found that this agent prolongs the duration of these events. This finding indicates that the insensitivity of $GABA_A$ receptors to ethanol is not due to a general lack of sensitivity of the receptors to

allosteric modulators. In addition, ethanol did not modulate the amplitude, decay, or frequency of spontaneous $GABA_A$ receptor-mediated PSCs in these cells. These findings suggest that acute ethanol exposure has neither a presynaptic effect nor a postsynaptic effect on $GABA_A$ receptor-mediated synaptic transmission at RSC neurons. Future experiments should investigate the reasons for the insensitivity of developing RSC neurons to the facilitatory effects of ethanol on GABA release, which may be due to differences in the properties of presynaptic ion channels, G protein-coupled receptors, and/or intracellular signaling pathways[39,40]. The results of our past and present studies on the effect of acute ethanol exposure support the notion that ethanol-induced cell death in the RSC is most likely triggered by inhibition of post-synaptic NMDA receptor function rather than potentiation of $GABA_A$ receptor-mediated neurotransmission either at the presynaptic or postsynaptic levels.

It has been demonstrated that third-trimester equivalent ethanol exposure results in long-term loss of INs in the rodent brain[13,41], including PV-INs in the RSC[17,42]. In Experiment #2, we demonstrate that binge-like ethanol exposure during this developmental period causes long-lasting alterations in the function of PV-IN→pyramidal neuron synapses. In ethanol exposed animals, oIPSCs decayed slower than in air-exposed controls, and had a larger area under the curve. We also observed sex by exposure condition interactions for decay time and decay constant, with male ethanol-exposed animals having oIPSCs that decayed much slower than those from air-exposed males. There were no post hoc effects of exposure condition in female mice, indicating that male animals may be more sensitive to the effects of third-trimester equivalent ethanol exposure. This is consistent with another study from our laboratory,

in which we showed that only male mice had reduced hippocampal IN survival after third-trimester equivalent ethanol exposure[13]. It is unlikely that changes in oIPSC kinetics are due to presynaptic alterations in probability of neurotransmitter release, as there was no effect of vapor-chamber exposure condition on paired-pulse ratios. Therefore, third-trimester equivalent ethanol exposure caused long-lasting postsynaptic modifications in $GABA_A$ receptor function. These functional changes could be due to long-lasting alterations in postsynaptic $GABA_A$ receptor subunit composition. During early postnatal development, α_2 containing $GABA_A$ receptors are predominantly expressed throughout the forebrain, while later in development α_1-containing $GABA_A$ expression is predominant[43]. $GABA_A$ receptors containing the α_2 subunit have slower decay kinetics than α_1 containing receptors[44]. Consequently, it is possible that developmental ethanol exposure impairs this $GABA_A$ subunit developmental switch. Future studies should systematically characterize the subunit composition of $GABA_A$ receptors expressed at PV-IN→pyramidal neuron synapses in layer V of the RSC to determine if they do indeed contain more α_2 subunits. Another interesting finding from this study concerns the reduction in oIPSC rise time in ethanol exposed animals. Alterations in rise-time can be indicative of changes in post-synaptic $GABA_A$ receptor subunit composition[45], receptor kinetics[46], GABA diffusion out of synaptic cleft[47] or synaptic vs. extra-synaptic receptor localization[48]. It is also possible that rise time was affected by dendritic filtering, as rise time increases as a function of distance of the synapse from the somatic recording location[49,50]. Determining the reason for ethanol-induced changes in rise time is an intriguing avenue for further investigation.

Recent studies that have examined the effect of developmental ethanol exposure on the function of INs. Delatour et al.[51] found that binge-like prenatal ethanol exposure (embryonic days 13.5 and 16.5) increases sIPSC frequency and charge transfer in layer V/VI pyramidal neurons of the somatosensory cortex of adolescent mice. These investigators also found an increase in the optically-evoked charge transfer paired-pulse ratios for IPSCs mediated by GABA release at PV-IN→pyramidal neuron synapses. The alterations in the charge transfer reported in that study are consistent with those we report here, indicating that this could be a common effect of ethanol exposure during the equivalents to the second and third trimesters of human pregnancy. Moreover, long-lasting disruptions in synaptic transmission at PV-IN→medium spiny neuron synapses in the dorsolateral striatum were detected in mice exposed to ethanol vapor during the equivalent to all trimesters of human pregnancy[52]. Taken together, our results and those of these electrophysiological studies propound the idea that deficits in the function of PV-INs could play a central role in the pathophysiology of FASD.

Deficits in learning and memory processes are among the most common negative consequences of developmental ethanol exposure[53]. Enhancement of post-synaptic GABAergic neurotransmission in the RSC after third-trimester equivalent ethanol exposure could have several impacts on parahippocampal network activity that may, in part, underlie the behavioral deficits observed in individuals with FASD. The RSC has reciprocal connections with several brain areas critical to learning and memory functions, including the hippocampal formation, the entorhinal cortex, and anterior/lateral thalamic nuclei[54]. Importantly, communication between the hippocampus and neocortex via sharp wave ripples involves a subiculum-RSC pathway[55].

Consequently, the RSC has a distinct role in spatial memory; it processes distal spatial cues and allows animals to orient themselves both spatially and directionally[56,57]. Lesioning or inactivating the RSC in rodents and macaques impairs performance on spatial memory tasks, while humans with damage to the RSC have problems with anterograde memory formation and navigation using spatial cues[54,58]. The contribution of PV-mediated GABAergic neurotransmission to RSC function and its role in spatial memory are poorly understood at present. However, recent work has demonstrated that PV-IN activity in the anterior cingulate cortex, to which the RSC is immediately posterior, is necessary for memory consolidation[59]. Given that the RSC and the anterior cingulate are adjacent and strongly interconnected[60], it is reasonable to hypothesize that a disruption in PV-IN-mediated signaling in the RSC will likewise impact learning and memory processes. Future work can test this hypothesis by capitalizing on advances in chemogenetic strategies to determine if up- or down-regulation of PV-IN activity impacts RSC physiology and/or performance on spatial memory tasks[58].

In conclusion, our findings indicate that third trimester-equivalent ethanol exposure has limited acute effects on postsynaptic $GABA_A$ receptor activity in the RSC but has an enduring impact on GABAergic transmission at PV-IN→pyramidal neuron synapses. Long-term alterations in postsynaptic $GABA_A$ receptor function caused by apoptosis of PV-INs in the RSC could contribute to some of the behavioral alterations observed in animal models of FASD[61]. Our findings suggest that detailed evaluation of the function of the RSC and related para-hippocampal cortical regions is warranted in humans with FASD.

ACKNOWLEDGEMENTS

Supported by NIH grants R37 AA015614 and P50 AA022534 (CFV); Undergraduate Pipeline Network Program and Maximizing Access to Research Career Programs (MJB). This research was partially supported by UNM Comprehensive Cancer Center Support Grant NCI P30CA118100 and made use of the Fluorescence Microscopy and Cell Imaging shared resource. We would like to thank Dr. Deidre Hill at the University of New Mexico Clinical & Translational Science Center for an initial consultation regarding the implementation of LMMs (supported by NIH grant UL1TR001449).

AUTHOR CONTRIBUTIONS

CWB and CFV designed experiments; CWB, GJC, MJB performed experiments; CWB, GJC, MJB analyzed data, CWB and CFV interpreted results and wrote the manuscript.

ETHICS DECLARATIONS

Competing interests

The authors declare no competing interests.

REFERENCES

1 Moore, D. B., Quintero, M. A., Ruygrok, A. C., Walker, D. W. & Heaton, M. B. Prenatal ethanol exposure reduces parvalbumin-immunoreactive GABAergic neuronal number in the adult rat cingulate cortex. *Neurosci Lett* **249**, 25-28, doi:10.1016/s0304-3940(98)00378-4 (1998).

2 Moore, D. B., Ruygrok, A. C., Walker, D. W. & Heaton, M. B. Effects of prenatal ethanol exposure on parvalbumin-expressing GABAergic neurons in the adult rat medial septum. *Alcohol Clin Exp Res* **21**, 849-856 (1997).

3 Bailey, C. D., Brien, J. F. & Reynolds, J. N. Chronic prenatal ethanol exposure alters the proportion of GABAergic neurons in layers II/III of the adult guinea pig somatosensory cortex. *Neurotoxicol Teratol* **26**, 59-63 (2004).

4 Miller, M. W. Effect of prenatal exposure to ethanol on glutamate and GABA immunoreactivity in macaque somatosensory and motor cortices: critical timing of exposure. *Neuroscience* **138**, 97-107 (2006).

5 Cuzon, V. C., Yeh, P. W., Yanagawa, Y., Obata, K. & Yeh, H. H. Ethanol consumption during early pregnancy alters the disposition of tangentially migrating GABAergic interneurons in the fetal cortex. *J Neurosci* **28**, 1854-1864, doi:10.1523/JNEUROSCI.5110-07.2008 (2008).

6 Skorput, A. G., Gupta, V. P., Yeh, P. W. & Yeh, H. H. Persistent Interneuronopathy in the Prefrontal Cortex of Young Adult Offspring Exposed to Ethanol In Utero. *J Neurosci* **35**, 10977-10988, doi:10.1523/JNEUROSCI.1462-15.2015 (2015).

7 Skorput, A. G., Lee, S. M., Yeh, P. W. & Yeh, H. H. The NKCC1 antagonist bumetanide mitigates interneuronopathy associated with ethanol exposure in utero. *Elife* **8**, doi:10.7554/eLife.48648 (2019).

8 Skorput, A. G. & Yeh, H. H. Chronic Gestational Exposure to Ethanol Leads to Enduring Aberrances in Cortical Form and Function in the Medial Prefrontal Cortex. *Alcohol Clin Exp Res* **40**, 1479-1488, doi:10.1111/acer.13107 (2016).

9 Larsen, Z. H. *et al.* Effects of Ethanol on Cellular Composition and Network Excitability of Human Pluripotent Stem Cell-Derived Neurons. *Alcohol Clin Exp Res* **40**, 2339-2350, doi:10.1111/acer.13218 (2016).

10 Granato, A. Altered organization of cortical interneurons in rats exposed to ethanol during neonatal life. *Brain Res* **1069**, 23-30, doi:10.1016/j.brainres.2005.11.024 (2006).

11 De Giorgio, A., Comparini, S. E., Intra, F. S. & Granato, A. Long-term alterations of striatal parvalbumin interneurons in a rat model of early exposure to alcohol. *J Neurodev Disord* **4**, 18, doi:10.1186/1866-1955-4-18 (2012).

12 Nirgudkar, P., Taylor, D. H., Yanagawa, Y. & Valenzuela, C. F. Ethanol exposure during development reduces GABAergic/glycinergic neuron numbers and lobule volumes in the mouse cerebellar vermis. *Neurosci Lett* **632**, 86-91, doi:10.1016/j.neulet.2016.08.039 (2016).

13 Bird, C. W., Taylor, D. H., Pinkowski, N. J., Chavez, G. J. & Valenzuela, C. F. Long-term Reductions in the Population of GABAergic Interneurons in the Mouse Hippocampus following Developmental Ethanol Exposure. *Neuroscience* **383**, 60-73, doi:10.1016/j.neuroscience.2018.05.003 (2018).

14 Coleman, L. G., Jr., Oguz, I., Lee, J., Styner, M. & Crews, F. T. Postnatal day 7 ethanol treatment causes persistent reductions in adult mouse brain volume and cortical neurons with sex specific effects on neurogenesis. *Alcohol* **46**, 603-612, doi:10.1016/j.alcohol.2012.01.003 (2012).

15 Sadrian, B., Lopez-Guzman, M., Wilson, D. A. & Saito, M. Distinct neurobehavioral dysfunction based on the timing of developmental binge-like alcohol exposure. *Neuroscience* **280**, 204-219, doi:10.1016/j.neuroscience.2014.09.008 (2014).

16 Saito, M. *et al.* Neonatal Ethanol Disturbs the Normal Maturation of Parvalbumin Interneurons Surrounded by Subsets of Perineuronal Nets in the Cerebral Cortex: Partial Reversal by Lithium. *Cereb Cortex* **29**, 1383-1397, doi:10.1093/cercor/bhy034 (2019).

17 Smiley, J. F. *et al.* Selective reduction of cerebral cortex GABA neurons in a late gestation model of fetal alcohol spectrum disorder. *Alcohol* **49**, 571-580, doi:10.1016/j.alcohol.2015.04.008 (2015).

18 Bird, C. W. *et al.* Neonatal ethanol exposure triggers apoptosis in the murine retrosplenial cortex: Role of inhibition of NMDA receptor-driven action potential firing. *Neuropharmacology* **162**, 107837, doi:10.1016/j.neuropharm.2019.107837 (2020).

19 Ikonomidou, C. *et al.* Blockade of NMDA receptors and apoptotic neurodegeneration in the developing brain. *Science* **283**, 70-74 (1999).

20 Ikonomidou, C. *et al.* Ethanol-induced apoptotic neurodegeneration and fetal alcohol syndrome. *Science* **287**, 1056-1060 (2000).

21 Olney, J. W. *et al.* Ethanol-induced apoptotic neurodegeneration in the developing C57BL/6 mouse brain. *Brain Res Dev Brain Res* **133**, 115-126 (2002).

22 Olney, J. W., Young, C., Wozniak, D. F., Jevtovic-Todorovic, V. & Ikonomidou, C. Do pediatric drugs cause developing neurons to commit suicide? *Trends Pharmacol Sci* **25**, 135-139, doi:10.1016/j.tips.2004.01.002 (2004).

23 Wang, Y. *et al.* Fluorescent labeling of both GABAergic and glycinergic neurons in vesicular GABA transporter (VGAT)-venus transgenic mouse. *Neuroscience* **164**, 1031-1043, doi:10.1016/j.neuroscience.2009.09.010 (2009).

24 Paxinos, G. & Franklin, K. B. J. *Paxinos and Franklin's The Mouse Brain in Stereotaxic Coordinates*. Fourth edn, (Elsevier, 2013).

25 Morton, R. A., Diaz, M. R., Topper, L. A. & Valenzuela, C. F. Construction of vapor chambers used to expose mice to alcohol during the equivalent of all three trimesters of human development. *J Vis Exp*, doi:10.3791/51839 (2014).

26 Schneider, C. A., Rasband, W. S. & Eliceiri, K. W. NIH Image to ImageJ: 25 years of image analysis. *Nat Methods* **9**, 671-675 (2012).

27 Ting, J. T. *et al.* Preparation of Acute Brain Slices Using an Optimized N-Methyl-D-glucamine Protective Recovery Method. *J Vis Exp*, doi:10.3791/53825 (2018).

28 Amrhein, V., Greenland, S. & McShane, B. Scientists rise up against statistical significance. *Nature* **567**, 305-307, doi:10.1038/d41586-019-00857-9 (2019).

29 West, B. T., Welch, K. B., Gałecki, A. T. & Gillespie, B. W. *Linear mixed models : a practical guide using statistical software*. Second edition. edn, (CRC Press, Taylor & Francis Group, 2015).

30 Golub, M. S. & Sobin, C. A. Statistical modeling with litter as a random effect in mixed models to manage "intralitter likeness". *Neurotoxicol Teratol* **77**, 106841, doi:10.1016/j.ntt.2019.106841 (2020).

31 Gelman, A. & Hill, J. *Data analysis using regression and multilevel/hierarchical models*. (Cambridge University Press, 2007).

32 Saito, M., Mao, R. F., Wang, R., Vadasz, C. & Saito, M. Effects of gangliosides on ethanol-induced neurodegeneration in the developing mouse brain. *Alcohol Clin Exp Res* **31**, 665-674 (2007).

33 Weiner, J. L. & Valenzuela, C. F. Ethanol modulation of GABAergic transmission: the view from the slice. *Pharmacol Ther* **111**, 533-554, doi:10.1016/j.pharmthera.2005.11.002 (2006).

34 Breese, G. R. *et al.* Basis of the gabamimetic profile of ethanol. *Alcohol Clin Exp Res* **30**, 731-744 (2006).

35 Sanderson, J. L., Donald Partridge, L. & Valenzuela, C. F. Modulation of GABAergic and glutamatergic transmission by ethanol in the developing neocortex: an in vitro test of the excessive inhibition hypothesis of fetal alcohol spectrum disorder. *Neuropharmacology* **56**, 541-555 (2009).

36 Galindo, R., Zamudio, P. A. & Valenzuela, C. F. Alcohol is a potent stimulant of immature neuronal networks: implications for fetal alcohol spectrum disorder. *J Neurochem* **94**, 1500-1511 (2005).

37 Zucca, S. & Valenzuela, C. F. Low concentrations of alcohol inhibit BDNF-dependent GABAergic plasticity via L-type Ca2+ channel inhibition in developing CA3 hippocampal pyramidal neurons. *J Neurosci* **30**, 6776-6781 (2010).

38 Sebe, J. Y., Eggers, E. D. & Berger, A. J. Differential effects of ethanol on GABA(A) and glycine receptor-mediated synaptic currents in brain stem motoneurons. *J Neurophysiol* **90**, 870-875, doi:10.1152/jn.00119.2003 (2003).

39 Kelm, M. K., Criswell, H. E. & Breese, G. R. Ethanol-enhanced GABA release: a focus on G protein-coupled receptors. *Brain Res Rev* **65**, 113-123, doi:10.1016/j.brainresrev.2010.09.003 (2011).

40 Roberto, M. & Varodayan, F. P. Synaptic targets: Chronic alcohol actions. *Neuropharmacology* **122**, 85-99, doi:10.1016/j.neuropharm.2017.01.013 (2017).

41 Ogievetsky, E., Lotfullina, N., Minlebaeva, A. & Khazipov, R. Ethanol-Induced Apoptosis of Interneurons in the Neonatal GAD67-GFP Mouse Hippocampus. *Bionanoscience* **7**, 151-154, doi:10.1007/s12668-016-0334-6 (2017).

42 Smiley, J. F. *et al.* Effects of neonatal ethanol on cerebral cortex development through adolescence. *Brain Struct Funct* **224**, 1871-1884, doi:10.1007/s00429-019-01881-1 (2019).

43 Fritschy, J. M., Paysan, J., Enna, A. & Mohler, H. Switch in the expression of rat GABAA-receptor subtypes during postnatal development: an immunohistochemical study. *J Neurosci* **14**, 5302-5324 (1994).

44 Lavoie, A. M., Tingey, J. J., Harrison, N. L., Pritchett, D. B. & Twyman, R. E. Activation and deactivation rates of recombinant GABA(A) receptor channels are dependent on alpha-subunit isoform. *Biophys J* **73**, 2518-2526, doi:10.1016/S0006-3495(97)78280-8 (1997).

45 Dixon, C., Sah, P., Lynch, J. W. & Keramidas, A. GABAA receptor alpha and gamma subunits shape synaptic currents via different mechanisms. *J Biol Chem* **289**, 5399-5411, doi:10.1074/jbc.M113.514695 (2014).

46 Banks, M. I., Li, T. B. & Pearce, R. A. The synaptic basis of GABAA,slow. *J Neurosci* **18**, 1305-1317 (1998).

47 Bier, M., Kits, K. S. & Borst, J. G. Relation between rise times and amplitudes of GABAergic postsynaptic currents. *J Neurophysiol* **75**, 1008-1012, doi:10.1152/jn.1996.75.3.1008 (1996).

48 Wu, X. *et al.* gamma-Aminobutyric acid type A (GABAA) receptor alpha subunits play a direct role in synaptic versus extrasynaptic targeting. *J Biol Chem* **287**, 27417-27430, doi:10.1074/jbc.M112.360461 (2012).

49 Henze, D. A., Cameron, W. E. & Barrionuevo, G. Dendritic morphology and its effects on the amplitude and rise-time of synaptic signals in hippocampal CA3 pyramidal cells. *J Comp Neurol* **369**, 331-344, doi:10.1002/(SICI)1096-9861(19960603)369:3<331::AID-CNE1>3.0.CO;2-6 (1996).

50 Galarreta, M. & Hestrin, S. Properties of GABAA receptors underlying inhibitory synaptic currents in neocortical pyramidal neurons. *J Neurosci* **17**, 7220-7227 (1997).

51 Delatour, L. C., Yeh, P. W. L. & Yeh, H. H. Prenatal Exposure to Ethanol Alters Synaptic Activity in Layer V/VI Pyramidal Neurons of the Somatosensory Cortex. *Cereb Cortex* **30**, 1735-1751, doi:10.1093/cercor/bhz199 (2020).

52 Cuzon Carlson, V. C., Gremel, C. M. & Lovinger, D. M. Gestational alcohol exposure disrupts cognitive function and striatal circuits in adult offspring. *Nat Commun* **11**, 2555, doi:10.1038/s41467-020-16385-4 (2020).

53 Mattson, S. N., Bernes, G. A. & Doyle, L. R. Fetal Alcohol Spectrum Disorders: A Review of the Neurobehavioral Deficits Associated With Prenatal Alcohol Exposure. *Alcohol Clin Exp Res* **43**, 1046-1062, doi:10.1111/acer.14040 (2019).

54 Vann, S. D., Aggleton, J. P. & Maguire, E. A. What does the retrosplenial cortex do? *Nat Rev Neurosci* **10**, 792-802, doi:10.1038/nrn2733 (2009).

55 Nitzan, N. *et al.* Propagation of hippocampal ripples to the neocortex by way of a subiculum-retrosplenial pathway. *Nat Commun* **11**, 1947, doi:10.1038/s41467-020-15787-8 (2020).

56 Mitchell, A. S., Czajkowski, R., Zhang, N., Jeffery, K. & Nelson, A. J. D. Retrosplenial cortex and its role in spatial cognition. *Brain Neurosci Adv* **2**, 2398212818757098, doi:10.1177/2398212818757098 (2018).

57 Todd, T. P., Fournier, D. I. & Bucci, D. J. Retrosplenial cortex and its role in cue-specific learning and memory. *Neurosci Biobehav Rev* **107**, 713-728, doi:10.1016/j.neubiorev.2019.04.016 (2019).

58 Milczarek, M. M. & Vann, S. D. The retrosplenial cortex and long-term spatial memory: from the cell to the network. *Current Opinion in Behavioral Sciences* **32**, 50-56 (2020).

59 Xia, F. *et al.* Parvalbumin-positive interneurons mediate neocortical-hippocampal interactions that are necessary for memory consolidation. *Elife* **6**, doi:10.7554/eLife.27868 (2017).

60 Corcoran, K. A., Frick, B. J., Radulovic, J. & Kay, L. M. Analysis of coherent activity between retrosplenial cortex, hippocampus, thalamus, and anterior cingulate cortex during retrieval of recent and remote context fear memory. *Neurobiol Learn Mem* **127**, 93-101, doi:10.1016/j.nlm.2015.11.019 (2016).

61 Lewin, M. *et al.* Developmental Ethanol-Induced Sleep Fragmentation, Behavioral Hyperactivity, Cognitive Impairment and Parvalbumin Cell Loss are Prevented by Lithium Co-treatment. *Neuroscience* **369**, 269-277, doi:10.1016/j.neuroscience.2017.11.033 (2018).

62 Lein, E. S. *et al.* Genome-wide atlas of gene expression in the adult mouse brain. *Nature* **445**, 168-176, doi:10.1038/nature05453 (2007).

Table 1: Characteristics of $GABA_A$-sPSCs before, during, and after 90 mM acute ethanol application in layer V pyramidal neurons and INs in the RSC of P6-P8 animals. Data are presented as mean(SEM). The frequency (hz), amplitude (pA), rise time (ms) and decay contant (tau) are presented during the baseline, 90 mM ethanol application, and washout phases separately for pyramidal neurons and INs. Repeated measures ANOVA effects with a p-value of < 0.05 are indicated with the following notations: C = cell-type effect, P = phase effect, and CxP = cell type by phase interaction. Male pyramidal n = 4 cells from 4 animals from 4 litters; female pyramidal = 4 cells from 4 animals from 3 litters; male IN = 4 cells from 4 animals from 4 litters, female IN = 3 cells from 3 animals from 2 litters.

		Pyramidal			Interneuron		
	Effects with p < 0.05	**Baseline**	**90 mM ethanol**	**Wash**	**Baseline**	**90 mM ethanol**	**Wash**
Frequency (Hz)	**C**	1.63(0.42)	1.91(0.42)	1.84(0.37)	0.28(0.12)	0.42(0.20)	0.42(0.15)
Amplitude (pA)	**P, CxP**	22.53(1.12)	21.76(0.73)	21.95(0.89)	18.84(1.66)	20.02(2.18)	24.96(3.17)
Rise time (ms)	**-**	3.07(0.27)	3.20(0.29)	3.24(0.30)	2.48(0.24)	2.76(0.37)	2.79(0.33)
Decay (tau)	**C**	23.39(2.01)	27.82(3.45)	24.85(2.83)	46.01(5.79)	48.60(5.98)	58.33(13.60)

FIGURE LEGENDS

Figure 1: Overview of electrode placement and timeline for the two experiments performed. a) Electrode placement and timeline for Experiment 1. The acute effects of ethanol and flunitrazepam on $GABA_A$ receptor mediated PSCs were measured in layer V pyramidal neurons and INs of the RSC. To electrically evoke $GABA_A$-PSCs, a bipolar stimulating electrode was placed on the border of layers I/II. b) Electrode placement, laser stimulation location, and timeline for Experiment 2. The long-term effects of P7 ethanol vapor chamber exposure were measured at P40-60. PV-INs expressing channel rhodopsin-2/tdTomato were stimulated with a 473 nm laser using a 40X objective lens in layer V of the RSC. Optically evoked IPSCs were recorded from in layer V pyramidal neurons. Atlas images were adapted from the Allen Brain Coronal Atlas https://mouse.brain-map.org/static/atlas[62]. Image credit: Allen Institute.

Figure 2: Effect of acute ethanol application on evoked $GABA_A$ receptor-mediated postsynaptic current ($GABA_A$-ePSC) amplitude and decay in layer V pyramidal neurons and INs. a) Average ePSC traces from layer V pyramidal neurons during the baseline (black trace) and acute 90 mM ethanol application (blue trace) phases. Scale bars = 40 ms,50 pA. b) Average ePSC traces from layer V INs during the baseline and acute 90 mM ethanol application phases. Scale bars = 40 ms, 20 pA. c) Normalized $GABA_A$-ePSC amplitudes for both pyramidal neurons (black circles) and INs (red squares) in layer V during the baseline, 90 mM ethanol application, washout, and GABAzine (25 µM) application phases. d) Normalized decay constants (tau) for both

pyramidal neurons and INs during the baseline, 90 mM ethanol application and washout phases. Data are presented as mean ± SEM.

Figure 3: Effect of acute flunitrazepam application on evoked $GABA_A$ receptor-mediated postsynaptic current ($GABA_A$-ePSC) amplitude and decay in layer V pyramidal neurons and INs. a) Average ePSC traces from layer V pyramidal neurons during the baseline (black trace) and acute 1µM flunitrazepam application (green trace) phases. Scale bars = 40 ms, 50 pA. b) Average $GABA_A$-ePSC traces from layer V INs during the baseline and acute 1µM flunitrazepam application phases. Scale bars = 40 ms, 20 pA. c) Normalized $GABA_A$-ePSC amplitudes for both pyramidal neurons (black squares) and INs (red squares) in layer V during the baseline, 1 µM flunitrazepam, washout, and GABAzine application phases. d) Normalized decay constants (tau) for both pyramidal neurons and INs during the baseline, 1 µM flunitrazepam, and washout phases. Data are presented as mean ± SEM.

Figure 4. Representative sPSC current traces from pyramidal neurons and interneurons demonstrating the effect of 90 mM ethanol and 25 µM gabazine bath applications in P7 brain slices. a) Representative average sPSC current trace from a pyramidal neuron before (baseline, black trace) and during 90 mM ethanol bath application (blue trace). b) Representative average sPSC current trace from an interneuron before and during 90 mM ethanol bath application. Scale bars for average traces = 25 ms, 5 pA. c) Representative compressed sPSC current trace from a pyramidal neuron during baseline (black trace), 90 mM ethanol bath application (blue

trace), and 25 µM gabazine application (purple trace) phases. d) Representative compressed sPSC current trace from an interneuron during baseline, 90 mM ethanol bath application, and 25 µM gabazine application phases. Scale bars = 4s, 20 pA. See Table 1 for average data.

Figure 5: Representative immunohistochemistry (IHC) images from B6 PV^{cre}-Ai27D mice and analysis of both penetrance and specificity of transgene expression. a-d) Representative IHC images showing colocalization of PV and ChR2-tdTomato. a) IHC demonstrating PV expression. b) Expression of endogenous ChR2–tdTomato transgene expression. c) DAPI nuclear stain. d) Merged image. Scale bar = 25 µm. e) Penetrance analysis of B6 PV^{cre}-Ai27D transgene expression. Penetrance of transgene expression was measured as the number of PV expressing cells colocalized with tdTomato divided by the number of PV expressing cells. f) Specificity analysis of B6 PV^{cre}-Ai27D transgene expression. Specificity of transgene expression was measured as the number of cells expressing only tdTomato divided by the number of cells expressing both PV and tdTomato. Air male n = 3 animals from 3 litters, air female n = 2 animals from 2 litters; ethanol male n = 3 animals from 3 litters, ethanol female n = 2 animals from 2 litters. Data are presented as mean ± SEM.

Figure 6: Effect of P7 ethanol exposure on optically-evoked inhibitory postsynaptic currents (oIPSCs) in layer V RSC pyramidal neurons at P40-60. a) Average oIPSC current traces from air-exposed animals using 0.5 ms (black trace) 1 ms (red trace) 2 ms (green trace) 4 ms (purple trace) and 8 ms (orange trace) laser pulse

durations. b) Average oIPSC current traces from ethanol-exposed animals using 0.5, 1, 2, 4, and 8 ms laser pulse durations. Scale bars = 20 ms, 200 pA. Blue arrows indicate onset of laser pulse. c-i) Collected peak amplitudes (c), current densities (d), GABAergic total charge (e),half widths at half-maximum amplitude (f), rise times (g), decay times (h), and decay time constants (tau) (i) for all cells from air exposed (black circles) and ethanol exposed (red squares) animals presented for each laser pulse duration. Dagger (†) denotes a p-value of < 0.06, and asterisks (*,**,***,****) denote p-values of $p < 0.05$, $p < 0.01$, $p < 0.001$, and $p < 0.0001$, respectively. LMM effects: E = exposure effect, L = laser pulse duration effect, S = sex effect, ExL = exposure by laser pulse duration interaction, ExS = exposure by sex interaction. The exposure by sex interaction for decay tau indicated in (i) is further explored in Supplemental Figure 2. Significance indicators next to x-axis laser pulse duration labels of panel e) indicate a Mann-Whitney U post hoc effect of exposure within laser pulse duration. Female air n = 32 cells from 8 animals from 7 litters, male air n = 46 cells from 9 animals from 8 litters; female ethanol n = 35 cells from 8 animals from 8 litters, male ethanol n = 40 cells from 8 animals from 7 litters. Data are presented as mean ± SEM.

Figure 7: Effect of P7 ethanol exposure on optically-evoked inhibitory postsynaptic currents (oIPSCs) paired-pulse ratios in layer V RSC pyramidal neurons at P40-60. a) Average oIPSC PPR current traces from air-exposed (black trace) and ethanol-exposed (red trace) animals, collapsed across sex. Amplitudes of traces from air- and ethanol-exposed animals are normalized to the amplitude of the first peak to illustrate PPRs. Scale bar = 40 ms. b) Collected amplitude PPRs for all cells

from air-exposed (black circles) and ethanol-exposed (red squares) animals. c) Collected total charge PPRs for all cells from air-exposed and ethanol-exposed animals. Asterisk (*) denotes a p-value of $p < 0.05$. S = sex effect. Air female n = 19 cells from 5 animals from 4 litters, air male n = 22 cells from 6 animals from 5 litters; ethanol female n = 22 cells from 6 animals from 5 litters; ethanol male n = 20 cells from 5 animals from 5 litters. Data are presented as mean ± SEM.

Figure 1

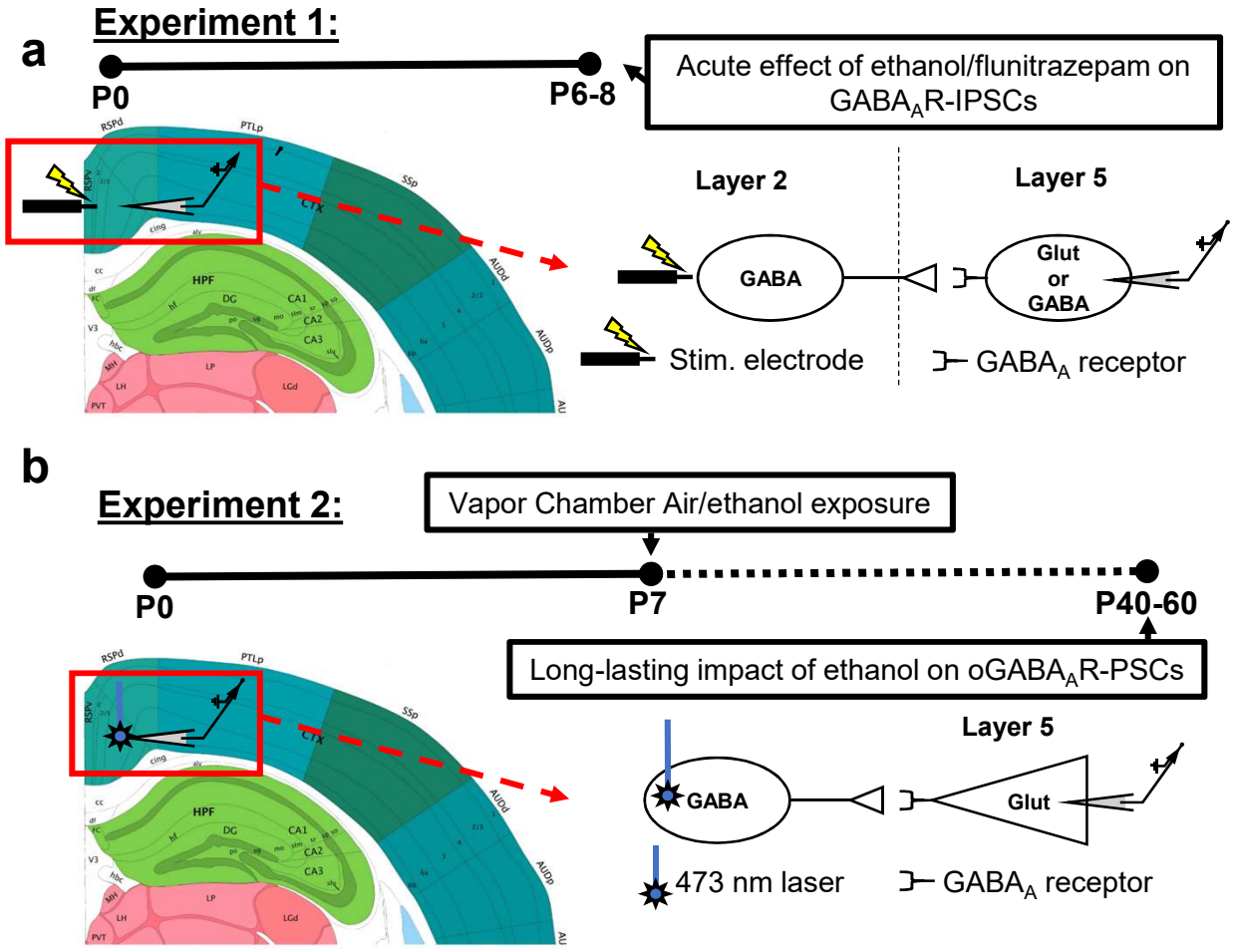

Figure 2

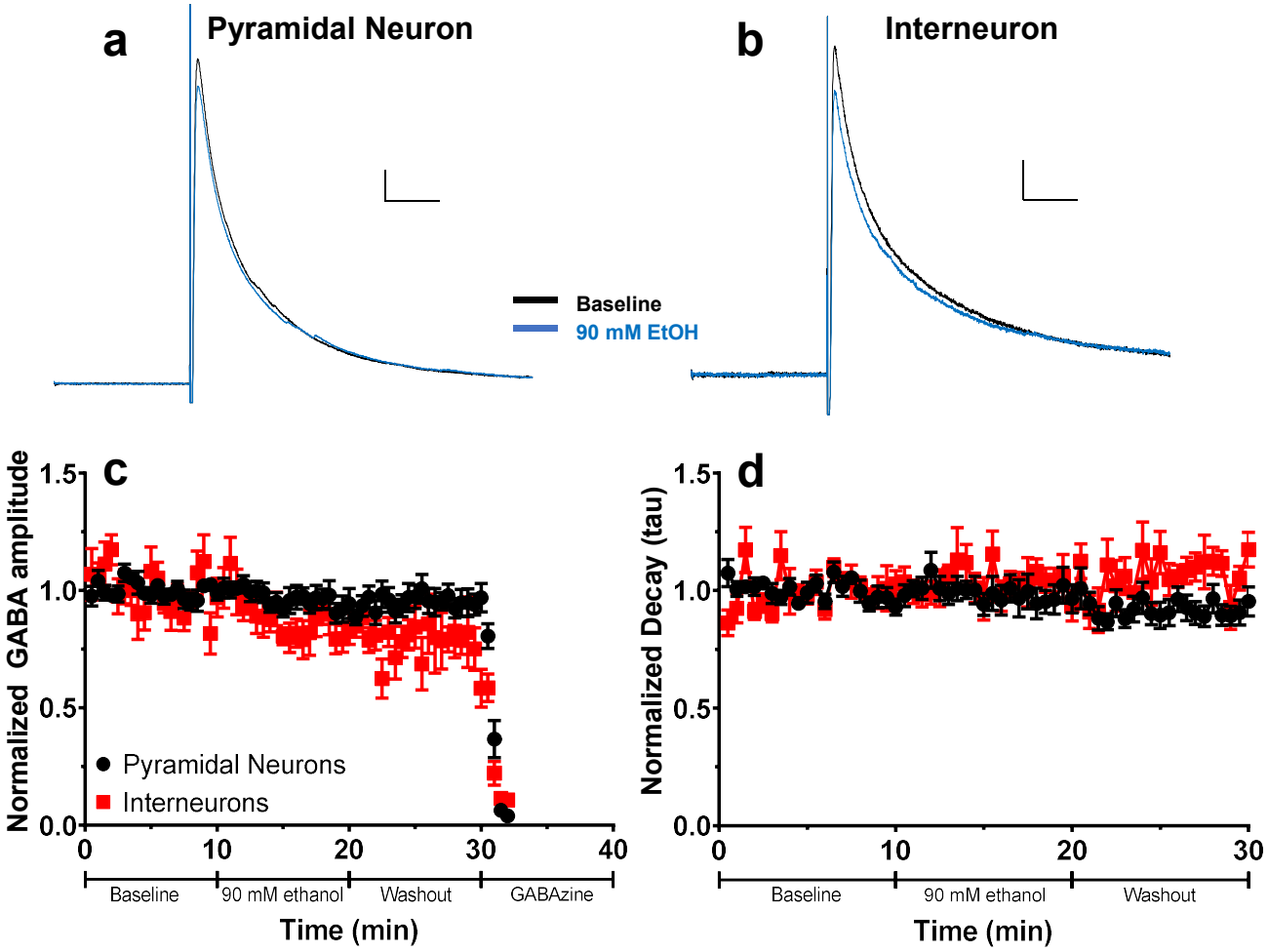

Figure 3

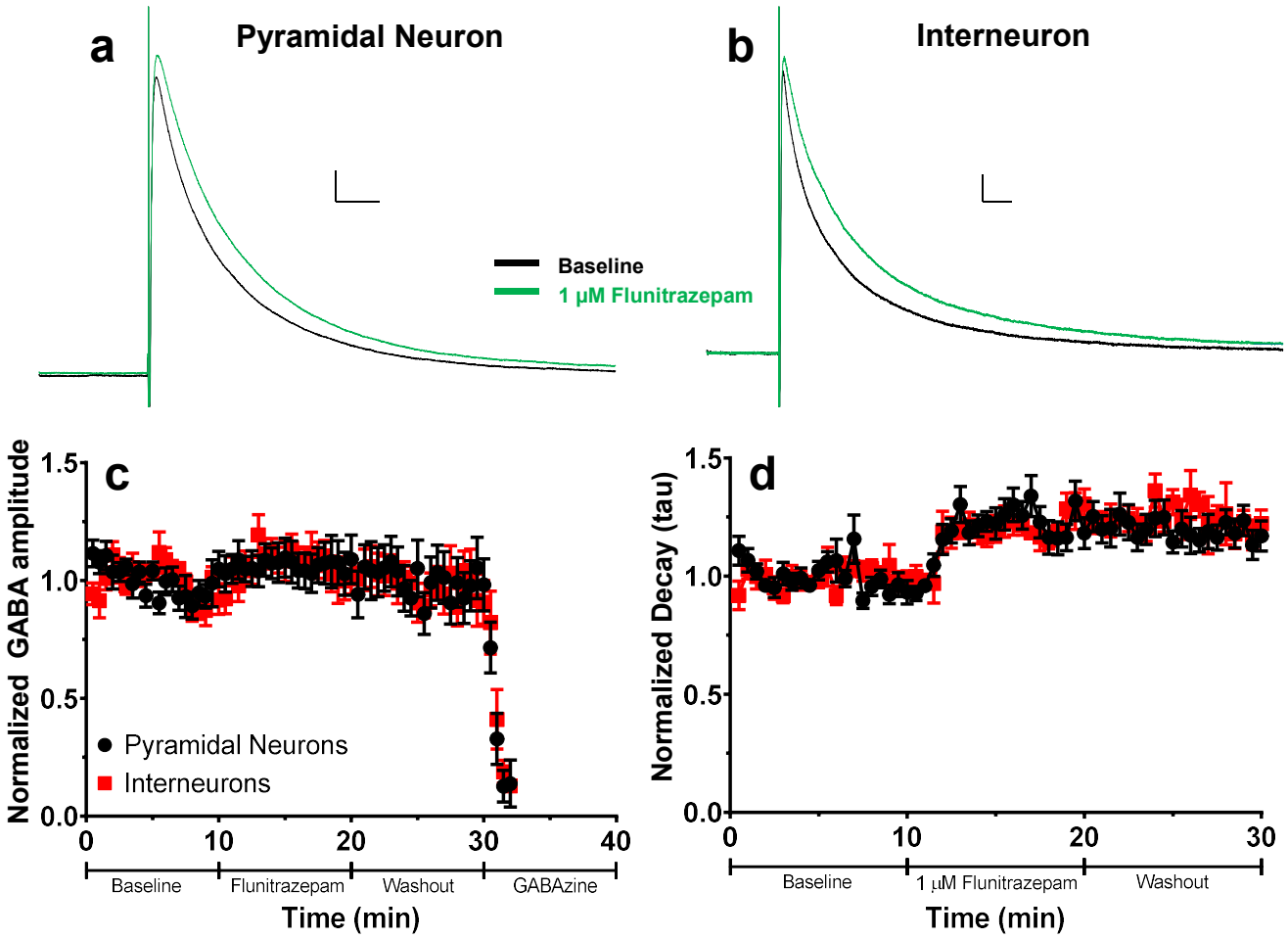

Figure 4

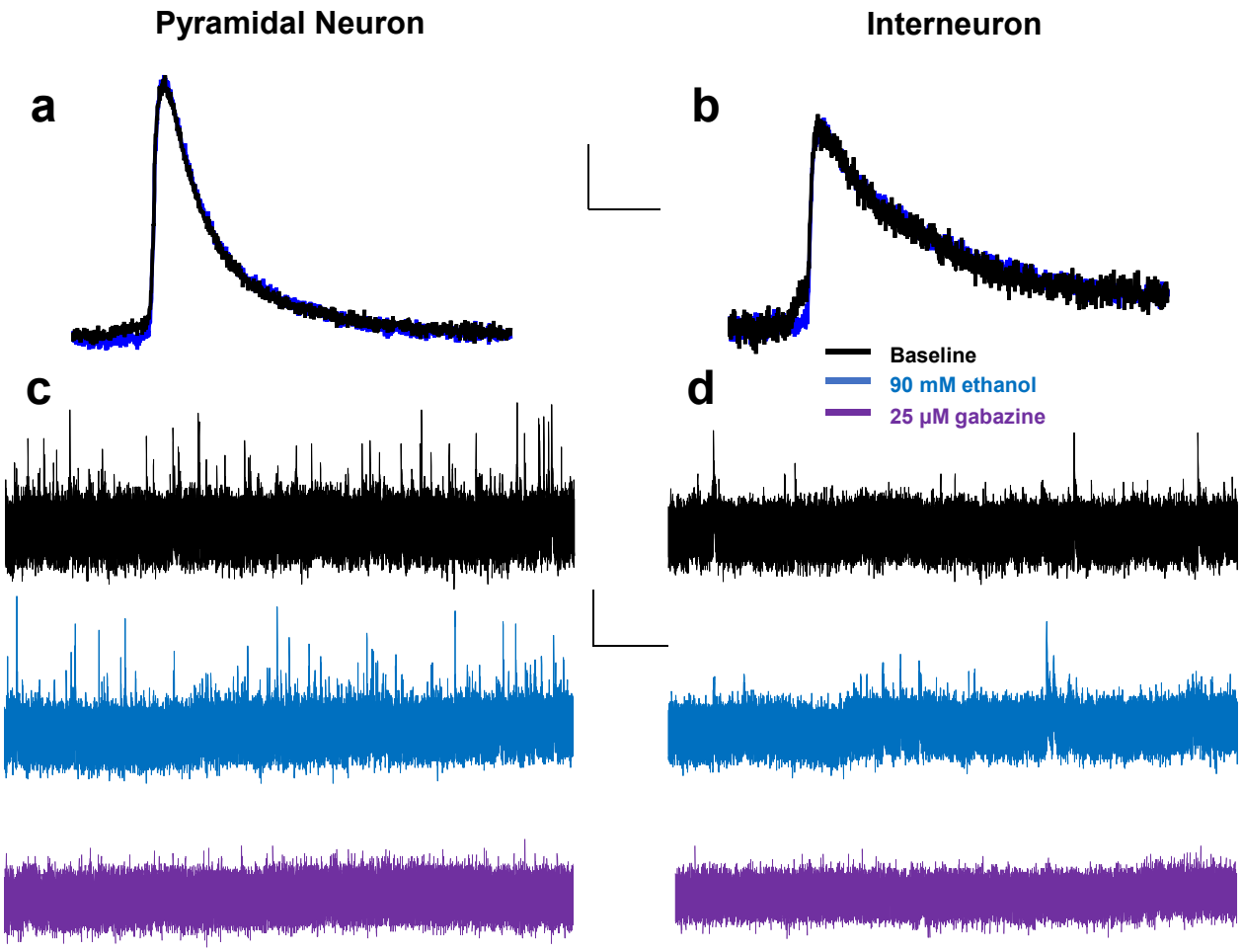

Figure 5

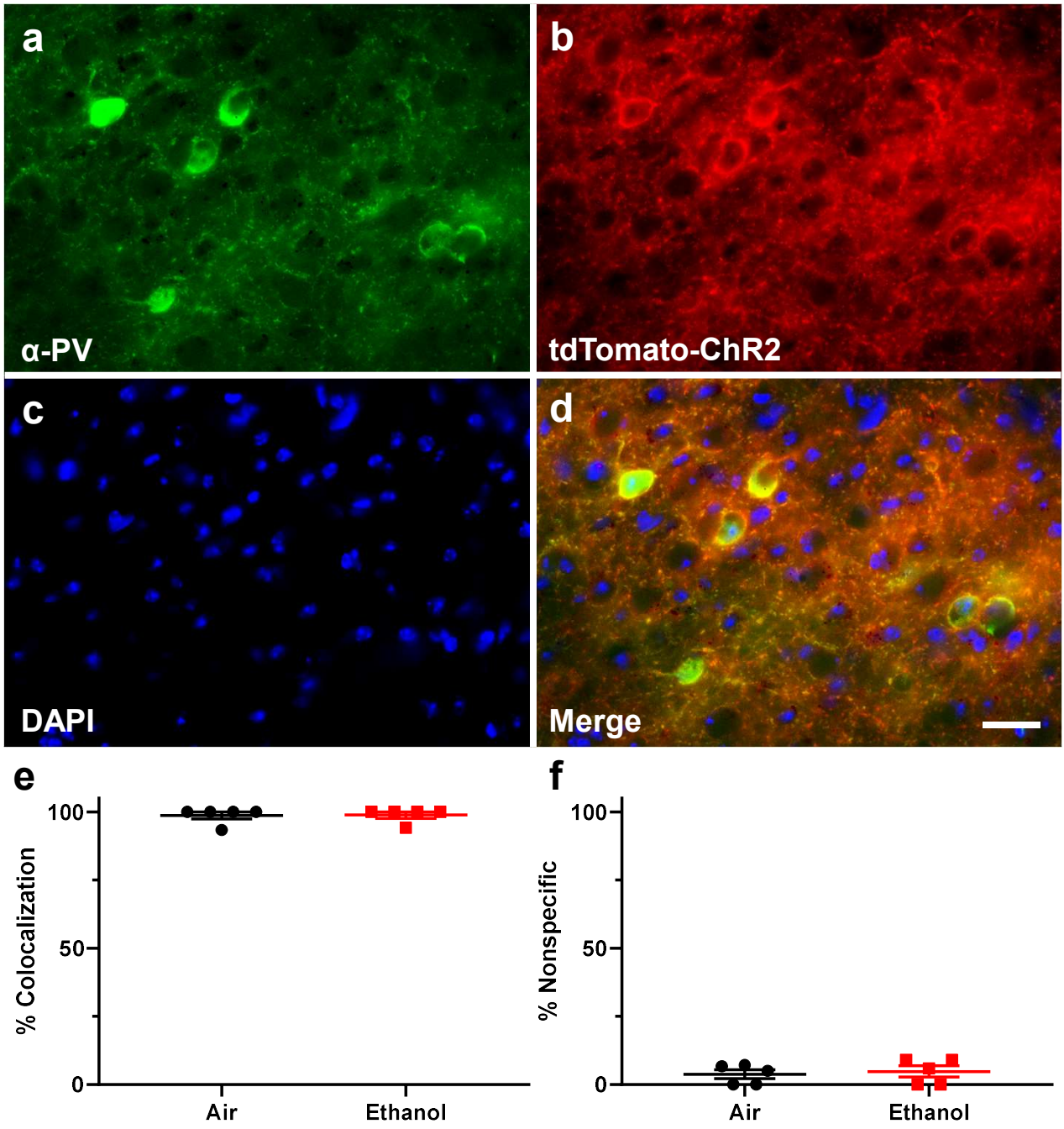

Scale bar 25 microns

Figure 6

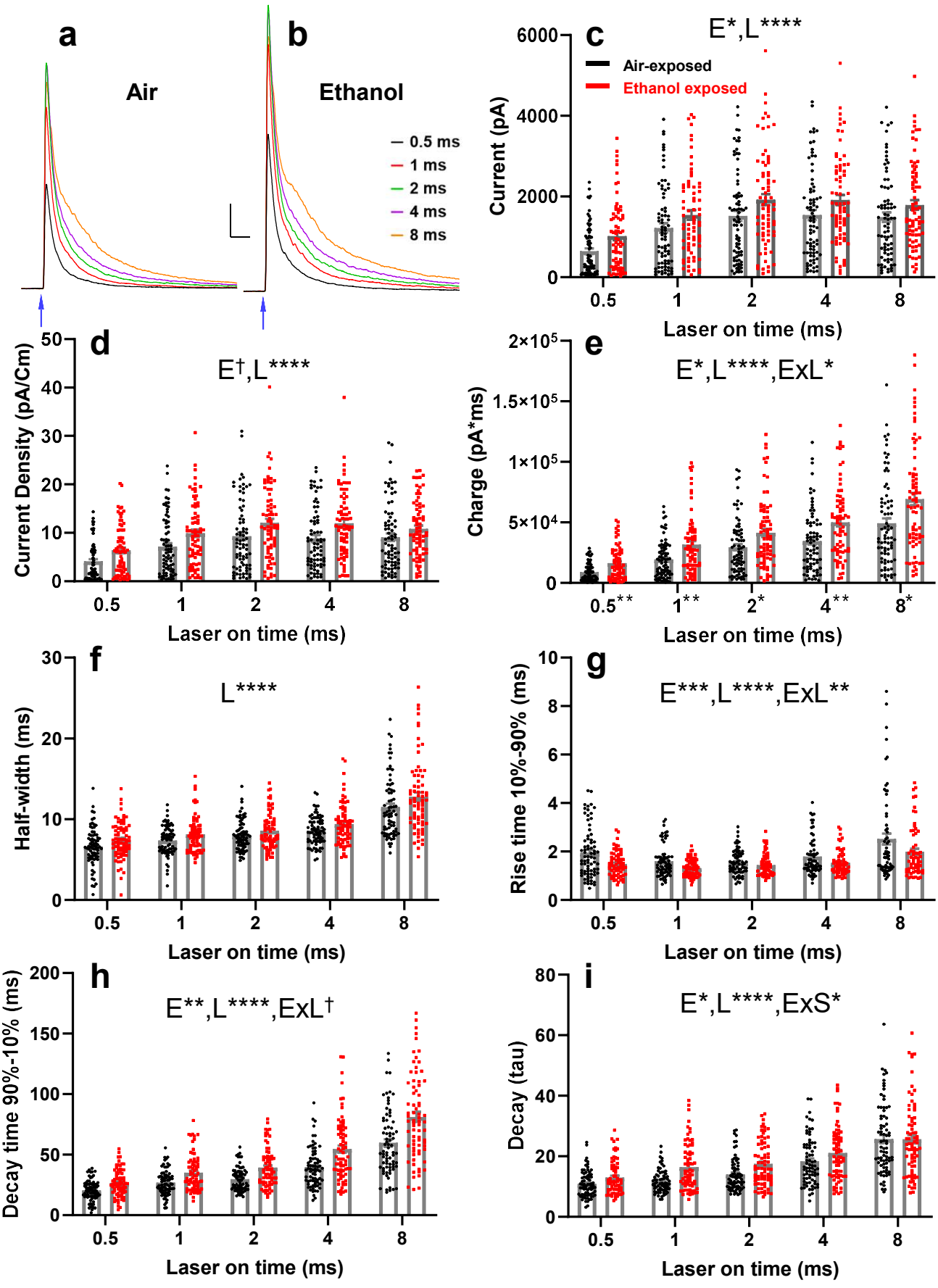

Figure 7